Calculations of crystal-structure stabilities of Ce under pressure

Olle Eriksson,* J. M. Wills, and A. M. Boring
Center for Materials Science, Los Alamos National Laboratory, Los Alamos, New Mexico 87545
and Theoretical Division, Los Alamos National Laboratory, Los Alamos, New Mexico 87545
(Received 18 February 1992; revised manuscript received 20 July 1992)

The total energies of the observed crystal structures of Ce [face-centered cubic (fcc), orthorhombic, and body-centered tetragonal (bct)] under pressure have been calculated, using the local-density approximation. The linear-muffin-tin-orbital calculations were full potential, all electron, and fully relativistic. The experimental data for the different crystallographic transitions are well reproduced by the calculations and we have extracted two terms that are mainly responsible for the $\alpha \rightarrow \alpha'$ transition: a one-electron term and a Madelung term. The $\alpha \rightarrow \alpha'$ transition is driven by the increasing importance of the $4f$ contribution with decreasing volume. This finding is also supported by a calculation without the $4f$ contribution to the cohesion which yields the α' phase unstable. The $\alpha' \rightarrow$bct transition is found to be somewhat more complex in nature since it is quite heavily influenced also by the $5d$ electrons. The calculated ground state is (correctly) found to be fcc and the equilibrium volume as well as the bulk modulus are in good agreement with experiment. The present *ab initio* calculation of a crystallographic phase diagram of an f electron system suggests delocalized $4f$ electrons exist in the high-pressure phases, including the α phase, of Ce.

INTRODUCTION

Cerium has a very interesting phase diagram.[1] At atmospheric pressure and low temperatures the enhanced Pauli paramagnetic α phase is stable [face-centered-cubic (fcc) structure]. With increasing temperature α-Ce transforms to the β phase (double hcp) and to the γ phase (fcc). The susceptibility of these two phases show Curie-Weiss behavior with an effective moment close to the free ion value, suggesting a localized $4f$ electron. At room temperature and a pressure of 7 kbar the trivalent low-density γ phase collapses into the much denser but isostructural α phase, with a decrease in volume of about 14%. A further increase in pressure transforms α-Ce to (orthorhombic) α'-Ce at $\sim$50 kbar[1,2] with a very small volume collapse. This phase is superconducting below 1.9 K.[3] With a further increasing pressure ($\sim$120 kbar), the orthorhombic α' phase transforms to a body-centered tetragonal phase (hereafter referred to as bct).[1-4] This phase is stable up to the highest experimentally studied pressures ($\sim$500 kbar).[1-4]

The underlying physical interactions driving the high-pressure phases (α, α', and bct) is the aim of the present work, and we argue that *these interactions have implications for the the entire phase diagram of Ce.* The α' phase is generally believed to be tetravelent.[1-4] The crystal structure of this phase is the same as for uranium (α-U) at low temperatures. The early actinides are known to have delocalized $5f$ electrons and it has been argued that the shape of the f spherical harmonic reflects the distorted crystal structures found for these elements. The similarity in crystal structure between α'-Ce and α-U can be taken as an indication that the $4f$ states in α'-Ce are itinerant. Similarly the crystal structure of elemental protactinium (Pa) is the same as the bct phase of Ce (although with a different c/a ratio). Hence some crystallographic phases of cerium are reminiscent of delocalized f-electron behavior.

Over the years there have been a number of models proposed to explain the isostructural $\gamma \rightarrow \alpha$ transition in Ce, but only a few are still compatible with all experimental data.[5-8] One model, the Mott transition model, suggests the $4f$ electrons localized and nonbonding in γ-Ce and itinerant and bonding in α-Ce.[9,7] This model is consistent with the positron experiments[7] and is supported by the fact that the band calculations of Glötzel[10] on the α phase of Ce yielded a theoretical volume in acceptable agreement with experimental data. A subsequent band calculation on Ce obtained similar results.[11] However, the calculations reported in Refs. 10 and 11 did not reproduce the observed volume collapse between γ- and α-Ce. Actually the γ phase was found to be energetically unstable.[10,11] However, by implementing the orbital polarization formalism[12] in a spin-polarized relativistic band calculation, thereby accounting for Hunds rules and allowing the possibility of one $4f$ orbital being completely filled and the rest empty, good account for the $\gamma \rightarrow \alpha$ transition was obtained.[13] The orbital polarization used in Ref. 13 introduced shifts of an $4f,m_l,\sigma$ orbital by an amount $-L^{\sigma}m_l E^3$, where L^{σ} is the orbital moment for the σ spin channel, m_l is the magnetic quantum number, and E^3 is the Racah parameter (calculated self-consistently). In this study it was found that the total energy was minimized when γ-Ce had one $4f$ orbital completely filled, and the rest empty—thereby describing localization (within this model), and that α-Ce has a $4f$ band pinned at the Fermi level. Furthermore, by including many-body correlations in a Kanamori-Hubbard formalism into a band scheme, it was found that the Coulomb interaction (U) necessary to localize a $4f$ elec-

tron in α-Ce is quite big (≥ 6 eV), whereas in γ-Ce a smaller U localizes a $4f$ electron (~ 5 eV).[14] Since an estimate of U for α-Ce is about 5 eV,[9,11] this model suggests that the $4f$ states are localized in γ-Ce but not in α-Ce. It was also found that the different contributions (hybridization or direct hopping) to the width of the $4f$ band are extremely anisotropic in k space, not additive, and about equally important.[14]

An alternative to the Mott model for the $\gamma \rightarrow \alpha$ transition has been suggested, namely, the Kondo volume collapse picture.[15] Both this model and the Mott model are consistent with most of the experimental data, indicating no change in the f-electron count (~ 1) upon making the transition. The Kondo volume collapse model, which has its energy scale and temperature dependence set by the experimental Kondo temperature T_K of the two phases, demonstrates that the spin quenching mechanism is consistent with other temperature-dependent data. It includes no change in the orbital moment through the transition. Moreover, the Kondo model differs from the Mott transition picture in that it describes the $4f$ electrons more localized (less delocalized) in the α phase. The $\gamma \rightarrow \alpha$ transition is here thought to be driven by differences in coupling between $4f$ electrons and the valence band. Although the $4f$ electrons contribute to the cohesion also in this model, this has been claimed to be in a different way than in the Mott model.[16]

At present, the Mott model[7,9,13] and the Kondo model[15] both contend in explaining the $\alpha \rightarrow \gamma$ transition and one concludes that *there are two conceptually different models that explain the $\alpha \rightarrow \gamma$ transition with equal accuracy.* However, we have in a previous communication pointed out that the high-pressure phases in Ce are *stabilized by the 4f electrons,* and that *the high-pressure phases of Ce, including the α phase, have itinerant 4f electrons.*[17] The conclusion that delocalized $4f$ electrons are crucial for determining the high-pressure phase diagram of Ce was earlier reached also by Skriver.[18] The present paper is a full report of our results on the crystallographic phase diagram of Ce, including energy bands, density of states, charge-density contour plots, and orbital occupation numbers. We have also performed simple model calculations to investigate the importance of hybridization versus direct hopping for determining the $4f$ bandwidth in Ce in a related way as was previously done.[14]

DETAILS OF THE CALCULATIONS

The total energy of Ce (per unit cell) is of the order of $-17\,717$ Ry/atom, while the difference in energy between the different phases is of the order of a few mRy/atom. Hence an accurate computational technique is required to study this transition. We used a full potential linear-muffin-tin-orbital (LMTO) technique[19] in the calculations reported here. The calculations were all electron, fully relativistic (with the spin-orbit coupling included at each variational step[20]), and employed no shape approximation to the charge density or potential. The base geometry was a muffin-tin geometry with a true interstitial; the basis functions, charge density, and potential were expanded in spherical harmonic series within the muffin tins and in Fourier series in the interstitial. The volume in the muffin-tin spheres was kept the same in both structures and was a fixed fraction (approximately 0.50) of the total volume. The basis set was comprised of augmented linear-muffin-tin orbitals.[20] The tails of the basis functions (the extension of the bases outside their parent spheres) were linear combinations of Hankel or Neuman functions with nonzero kinetic energy; three tail functions were used for each basis. The coefficients were chosen for each (n,l) value by fitting to atomic wave functions calculated from self-consistent potentials; the kinetic energies of the tail functions were chosen to optimize the fit. The basis set contained $5s$, $5p$, $6s$, $6p$, $5d$, and $4f$ orbitals; all orbitals were contained in the same energy panel with a separate set of energy parameters for the pseudovalence and the valence states. Approximate orthogonality between bases with the same l value was maintained by energy separation.

Integration over the Brillouin zone was done using "special point" sampling.[21] The results reported here used 10 points in the irreducible wedge of the α-Ce Brillouin zone and, correspondingly, 16 points in the irreducible wedge of the α'-Ce Brillouin zone and 58 points in the irreducible wedge of the body-centered tetragonal zone. The difference in energy between the different structures was found to be converged to less than 0.1 mRy by performing calculations at volumes near the transition volumes using sets containing from 10 to 60 points for α-Ce and between 16 and 128 points for α'-Ce and between 58 and 80 points for bct Ce. Spherical harmonic expansions were carried out through $l=8$ for the bases, charge density, and potential. The Fourier series for the basis functions contained 369 plane waves for α-Ce, 489 plane waves for bct Ce and 1053 plane waves for α'-Ce; the Fourier series for the charge density and potential contained 1695 plane waves for α-Ce, 2255 plane waves for bct Ce, and 5175 plane waves for α' Ce. Finally, the calculations used the Hedin-Lundqvist exchange-correlation functional.

TOTAL ENERGY RESULTS

Among the studied structures the fcc and bct phases are quite simple and we used the experimental c/a ratio for the bct phase. However the α' phase is somewhat more complicated. α'-Ce may be described as a one-face-centered orthorhombic lattice with two atoms per unit cell at positions (0,0,0) and $(0,0.5,1-2y)$ in units of the a, b, and c lattice translation vectors. The lattice constants are known but the value of $2y$ is not known experimentally. As a preliminary to calculating the equation of state of α'-Ce we performed a set of calculations to find the minimum in the total energy as a function of $2y$, using experimental values for the lattice constants at a volume close to the experimental transition volume (22.3 Å per atom). The minimum energy was found at $2y=0.225$ [Skriver's calculated value was 0.21 (Ref. 18)]; this value, together with the experimental ratios of the lattice constants, was then used at all volumes in calculating the equation of state of the α' phase. The theoretical value $2y=0.225$ may be compared with the value

$2y \cong 0.21$ found experimentally in the isostructural α phase of uranium.

The main result of this work—the total energy as a function of volume for the observed phases of Ce—is displayed in Fig. 1. The important features of Fig. 1 have been collected in Table I. At zero pressure, the structure of Ce is correctly found to be fcc with an equilibrium volume of 28.1 Å^3, which compares well with experimental results [$\sim$28–29 Å^3 (Refs. 1–4)]. Our calculated equilibrium volume agrees well with the value obtained from previous fully relativistic calculations,[13] whereas the scalar relativistic calculations of Ref. 11 underestimated the volume by $\sim$17%, and the scalar relativistic calculations of Glötzel[10] underestimated the volume by $\sim$13%. The fact that our calculations include the spin-orbit coupling as well as treating the 5*s* and 5*p* orbitals as (pseudo) valence states might explain this difference. Also, experience shows that using a larger (better converged) muffin-tin-orbital basis set, a so-called double basis set,[19] normally predicts a lower theoretical equilibrium volume (by a few percent) and this is possibly part of the reason for the disagreement between our calculated volume and the linear augmented plane wave (LAPW) results (these calculations used a larger basis than ours).[11] The calculated bulk modulus B at the experimental volume is 370 kbar, which may be compared with the experimental room-temperature value of $\sim$240–290 kbar.[1–4] The pressure derivative of B, called B', was calculated to be 4.4, in fair agreement with the experimental value 5.5.[1–4] We find a transition to the α' phase at a volume of 24.2 Å^3. The calculated volume collapse is quite small $\sim$1 Å^3 and the calculated transition pressure is 70 kbar. (The transition pressure may be obtained from the slope of the common tangent of the total energy curves in Fig. 1.) These values compare well with the experimental data reported for the $\alpha \rightarrow \alpha'$ transition, a transition volume of $\sim$24 Å^3,[1–4] accompanied by a small volume collapse and a transition pressure (extrapolated from the phase diagram to zero temperature) of $\sim$65 kbar.[1–4] To illustrate the delicacy of the calculations, we note that at the calculated equilibrium volume, the orthorhombic structure has a total energy $\sim$3 mRy/atom higher than the fcc structure while, as mentioned above, the total energy is $\sim -17\,717$ Ry/atom. Notice from Fig. 1 that at even smaller volumes ($\sim$20 Å^3) the α' phase transforms to the bct phase. The calculated pressure for this transition is 150 kbar and is also in good agreement with experimental data, 120 kbar at room temperature.[1–4] As is obvious from Fig. 1, this transition is even more delicate than the $\alpha \rightarrow \alpha'$ transition, since the energy difference between the bct and the α' phase is extremely small.

TABLE I. Calculated equilibrium volume and bulk modulus for α-Ce, as well as volumes, volume changes, and pressure for the $\alpha \rightarrow \alpha'$ and $\alpha' \rightarrow$bct transitions.

V_{eq} (Å^3)	28.1
B_{eq} (kbar)	370
$V\alpha \rightarrow \alpha'$ (Å^3)	24.2
$\Delta V\alpha \rightarrow \alpha'$ (Å^3)	1.0
$P\alpha \rightarrow \alpha'$ (kbar)	70
$V\alpha' \rightarrow$bct (Å^3)	20.0
$\Delta V\alpha' \rightarrow$bct (Å^3)	0.0
$P\alpha' \rightarrow$bct (kbar)	150

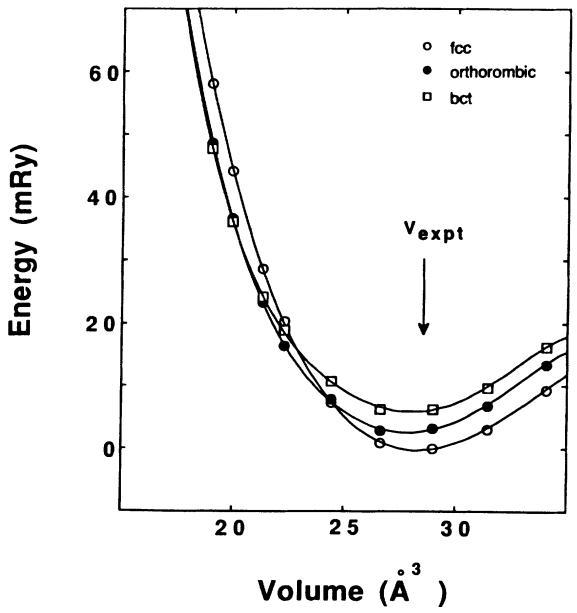

FIG. 1. Calculated total energy of α (fcc, open circles), α' (orthorhombic, filled circles), and bct (open squares) Ce. The calculated pressures for the phase transitions are obtained from the slope of the common tangent of the energy curves. The energies refer to the minimum energy of the fcc phase.

ELECTRONIC STRUCTURE

It is desirable to analyze the different contributions to the total-energy expression in order to see if certain terms are mainly responsible for the crystallographic transitions shown in Fig. 1. However, before attempting this it is illustrative to study the electronic structure, namely, the density of states (DOS) and the energy bands. In Fig. 2 we display our calculated DOS for two different volumes, 34.06 Å^3 [Fig. 2(a)] and 19.96 Å^3 [Fig. 2(b)]. The shaded area represents the 4*f* partial DOS. The α' phase has two atoms per cell. However, the partial DOS for the two different atom types are almost identical, and therefore we have plotted the partial DOS for one of them only. Notice that the sharp features of the DOS (Van Hove singularities) in the fcc phase gradually disappear when the symmetry of the structure is lowered (fcc$\rightarrow$bct$\rightarrow$orthorhombic). The electronic structure is seen to be dominated by the 4*f* contribution and the Fermi level cuts the 4*f* band at the low-energy side for all structures. The bandwidths are seen to be quite the same for all three structures, whereas the details of the DOS differ. Notice also that the 4*f* bandwidth is about three times broader for the lower volume. From Fig. 2 alone it is hard to see why one crystal structure should be favored over the other. The hybridization at the two volumes seems to be about the same, and the occupied part of the

DOS has about the same shape, although the low volume DOS is, of course, broader.

It is equally hard to argue for the change in crystal structures by looking at the bands. In Figs. 3(a) and 3(b) we show the bands corresponding to the DOS plotted in Fig. 2. The general interest for plotting bands has diminished lately, since, for instance, by studying the bands alone it is hard to argue why different crystal structures should be stable. However, with the new experimental techniques, which actually measure the energy dispersion (angle-resolved photoemission), we feel that it is of interest to display this dispersion. Therefore, the bands in Fig. 3 for the three different crystal structures make a comparison between theoretical and experimental energy dispersion possible.

However, one should bear in mind that previous experience[10,11,22,23] shows that the calculated DOS of α-Ce do not resemble the experimental spectra. More recent studies show that this to some extent is a surface effect, since it was demonstrated that the surface of α-Ce is γ-like,[24] in agreement with predictions.[25] Even when accounting for these surface effects and extracting the bulk signal of the photoelectron spectra, the agreement between calculated DOS functions and experiment is not satisfactory, suggesting a more complicated picture with the possibility of complex final-state effects, and so on.

For both volumes and for all structures the bands can be characterized by having a set of very narrow states lying just above E_F. These states have mostly $4f$ character and it is these states that give rise to the high peak just above E_F in the DOS (Fig. 2). Notice that the broadening and increasing dispersion of the $4f$ states with decreasing volume is about the same for the three structures. This is compatible with the DOS results presented in Fig. 2. Notice also that the lowest-lying energy band shows some peculiarities. It is expected that with decreasing volume an increase of the bandwidth should take place. However, our results show a counterintuitive effect for certain k points. For instance, at the Γ point, the lowest band in both the fcc and bct structures has an

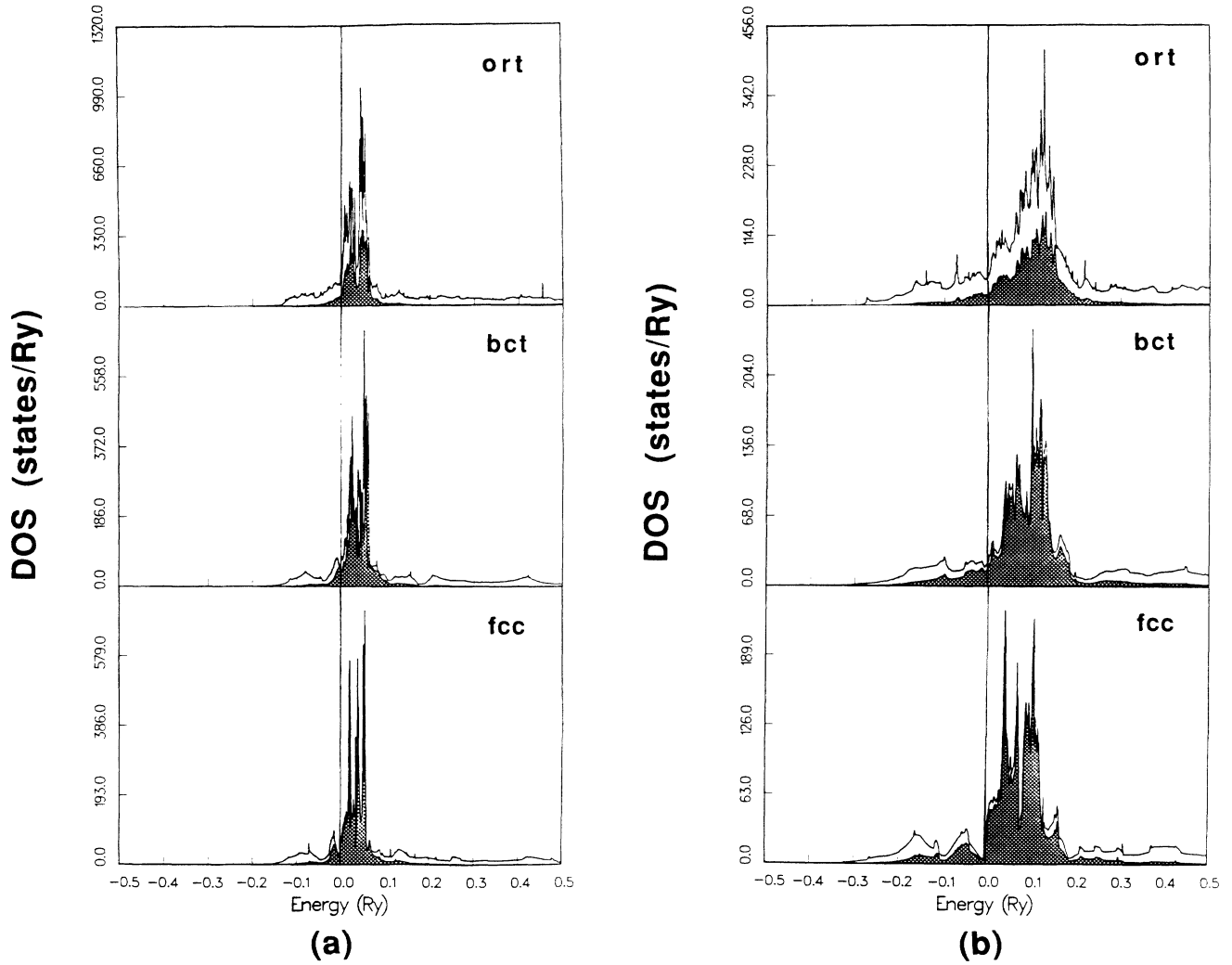

FIG. 2. Density of states (DOS) for fcc, bct, and orthorhombic Ce. The shaded area represents the $4f$ partial DOS. Energies are in Ry and the Fermi level is at zero energy and is marked with a vertical line. The DOS are plotted for two volumes 34.06 Å^3 (a) and 19.96 Å^3 (b).

energy of about -3.5 eV below E_F at the highest volume and an energy of about -1.5 eV below E_F for the lower volume. Similarly, in the orthorhombic structure the eigenvalue at the Γ point is more or less volume independent. This is only found for certain k points; the overall bandwidth (summed over the entire k space) is increasing with decreasing volume (Fig. 2). The reason for this counterintuitive effect is that with decreasing volume the s band is pushed up to higher energies relative to the d and f bands. For instance, for the high volume case the lowest eigenvalue at the Γ point is an s state. For the low volume case this s state is moved up in energy just below the next state, which is an f state. The lowest eigenvalue at the X point has mainly d character, and since the d band does not move up in energy, but broadens with decreasing volume, the lowest eigenvalue is moved from the Γ to the X point with increasing pressure. This effect has been observed for transition metals, where it is referred to as an $s \rightarrow d$ transfer.[26]

Notice also that the narrow $4f$ bands are dispersed about the same along the different symmetry lines, with the exception of the bct phase, which shows very little dispersion between the Z and Γ point. These points are along the z axis in k space, and thus this finding indicates that there is little interaction between the $4f$ electrons along the z axis of the bct lattice. This simply reflects the

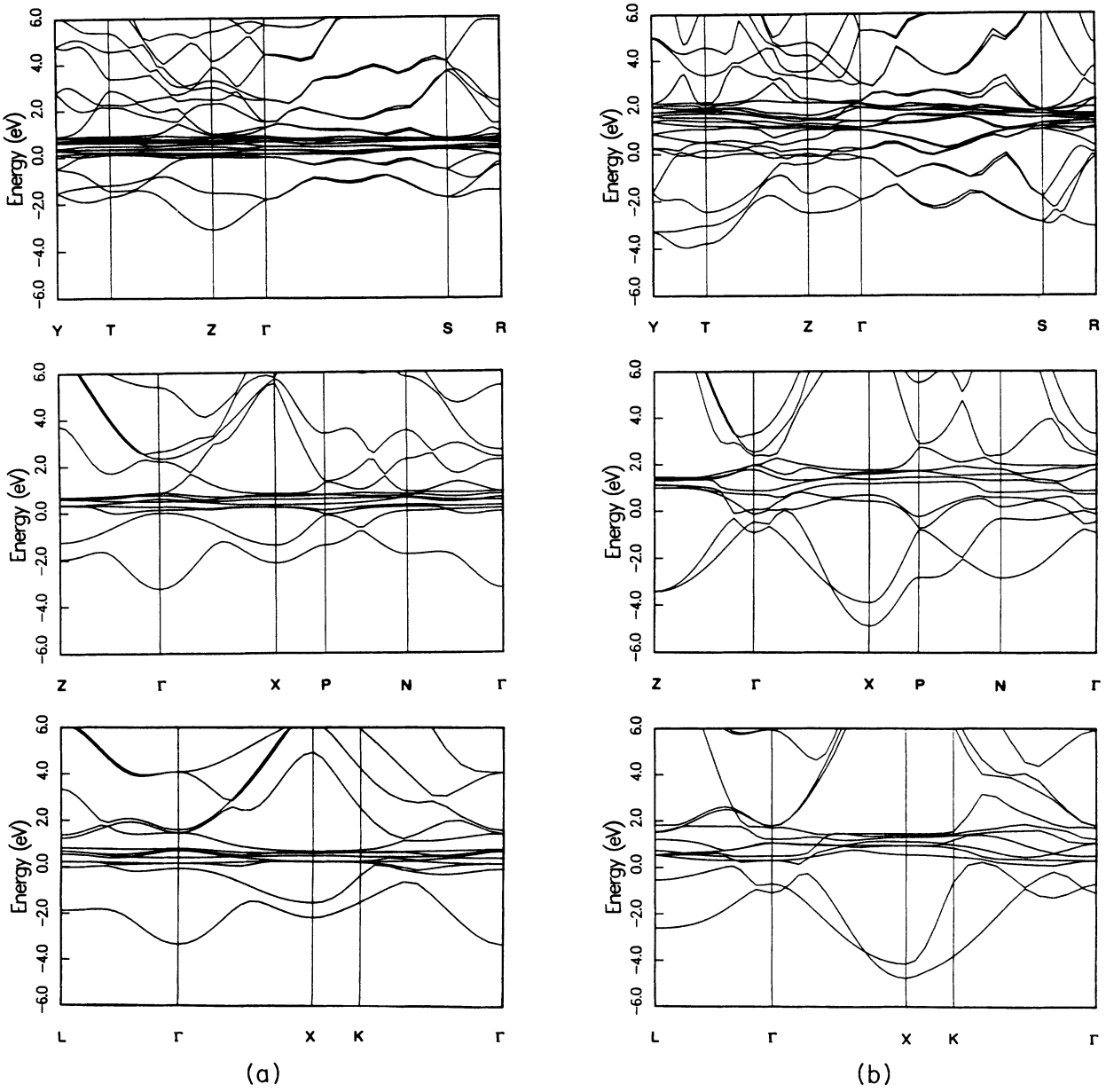

FIG. 3. Energy bands for fcc (lower panel), bct (middle panel), and orthorhombic (upper panel) Ce along high-symmetry directions. Energies are in eV and the Fermi level is at zero energy. The energy bands are plotted for two volumes 34.06 Å^3 (a) and 19.96 Å^3 (b).

fact that the interatomic spacing along this axis is quite large for this structure. Finally, we point out that the two lowest bands at the Z point in bct Ce are not degenerate, although at the smaller volume they are very close in energy.

TRIVALENT AND TETRAVALENT *spd* CALCULATION

The results presented above were obtained with the $4f$ electrons contributing to the bonding. This suggests that in order to account for a very delicate quantity, such as the crystal structure, it is important to treat the $4f$ states as bands. To test the importance of the $4f$ states for determining the crystal structures of Ce, we recalculated the total energy of Ce in the α, bct, and α' structures at a volume where it is known that Ce is in the α' phase (~ 22 Å^3), but with the $4f$ band being forced to be empty (using s, p, and d partial waves only). We have done this test calculation assuming three as well as four valence electrons. We performed calculations for both cases since it previously has been suggested that the high-pressure phases of Ce are tetravalent (four valence electrons), whereas more recent calculations reveal that the charge occupation in Ce, also at the higher pressures, is close to one (see below). This latter finding suggests that a calculation that forces the $4f$ bonding to be absent should be done using three valence electrons with the $4f$ electron treated as a core state.

As stated above we have tried both cases. For the tetravalent calculation we found bct to be the stable phase, with the α phase ~ 10 mRy and the α' phase ~ 20 mRy higher in energy, whereas for the trivalent calculation we found the bct phase to be stable with ~ 1 mRy lower energy than the α structure and ~ 10 mRy lower energy than the α' structure. This shows that at volumes where it is known from experiment that the orthorhombic structure is stable, treating Ce as a normal trivalent or tetravalent element is incorrect, and that the $4f$ electrons participate in the bonding and the formation of the crystal structure. This is consistent with the fact that certain features in the phase diagram, i.e., the $\alpha \rightarrow \alpha'$ transition, is not seen in other systems that do not have itinerant f electrons, e.g., Y or Zr.

ENERGY ANALYSIS

The results presented above show that it is necessary to treat the $4f$ electrons as bands in the high-pressure phases. This is further supported by additional analysis of the results of our calculations, since it was evident that the transition from the α to the α' phase was correlated with a balance of two competing terms in the total energy: a Madelung term, and a $4f$ one-electron eigenvalue term. The latter was calculated from the first moment of the $4f$ partial DOS. The Madelung term, which may be expressed approximately[27] as

$$E_M = -\tfrac{1}{2}(Q_I e)^2 \frac{\beta_M}{S_W} , \quad (1)$$

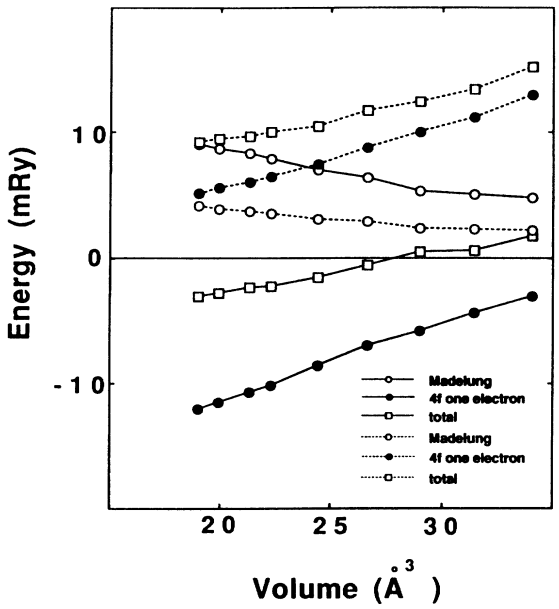

FIG. 4. Calculated difference $\alpha' - \alpha$ (solid lines) and bct-α (dotted lines) of the Madelung (open circles) and $4f$ one-electron (filled circles) contributions to the total energy, as well as their sum (open squares).

where β_M is the Madelung constant, S_W is the Wigner-Seitz radius, and Q_I is the interstitial charge, favors the close-packed α structure (Fig. 4). However, as seen in Fig. 4, the $4f$ terms favors the open α' structure. An obvious argument for this is that degeneracies in the partially occupied $4f$ bands may be broken by lowering the crystal symmetry. Occupied degenerate states in the fcc

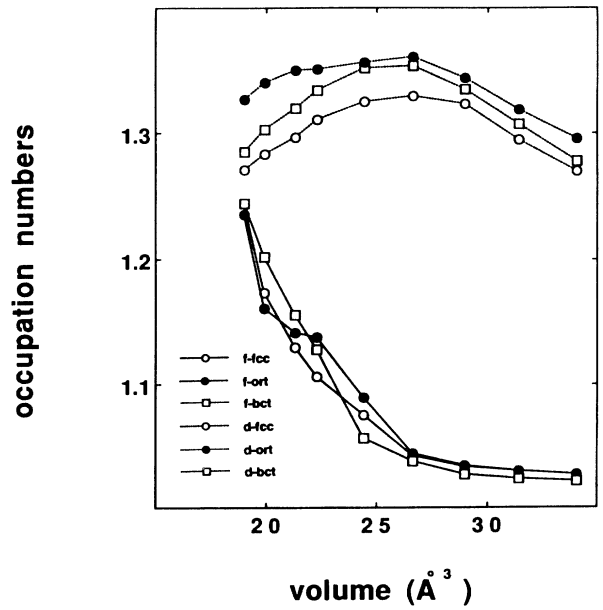

FIG. 5. $4f$ (full drawn lines) and $5d$ (dotted lines) occupation numbers for fcc (open circles), bct (open squares), and orthorhombic (filled circles) Ce.

phase that are close to E_F can therefore lower the total energy by lowering the crystal symmetry, since by doing this one band is pushed up above E_F (and therefore not affecting the total energy) and one band is pushed down, lowering the total energy. In Fig. 4, we also show the calculated sum of the Madelung and $4f$ one-electron terms (the curve labeled "total").[28] It is evident from Fig. 4 that the $\alpha \rightarrow \alpha'$ transition may be considered to be driven by the $4f$ eigenvalue sum: with increasing pressure the $4f$ term becomes increasingly important, and at a sufficiently high pressure, dominates the Madelung term, and the α' phase becomes stable. (Isolating only two contributions that drive the transition is, of course, a simplification, and the transition volume given in Fig. 4 is slightly larger than the one given in Fig. 1.)

We have also performed a similar energy analysis of the $\alpha' \rightarrow$bct phase transitions. However, as seen in Fig. 4 the interactions driving this transition are more complicated than the ones driving the $\alpha \rightarrow \alpha'$ transition. By isolating only the Madelung and $4f$ one-electron contribution to the total energy, we obtain the bct phase to be unstable at all volumes. The fact that the s, p, d calculations, presented in the previous section, yield the bct phase stable suggests that the interactions driving the bct phase in Ce also have non-$4f$ contributions (i.e., $5d$). Notice from Fig. 4 that with decreasing volumes and an increasing $4f$ bandwidth, the energy difference between the bct and fcc phases becomes smaller. However, notice also that with decreasing volume the energy difference between the α' and bct phase is more or less constant, and thus the $\alpha' \rightarrow$bct transition would not occur if no other terms played a role. As a matter of fact, for the bct

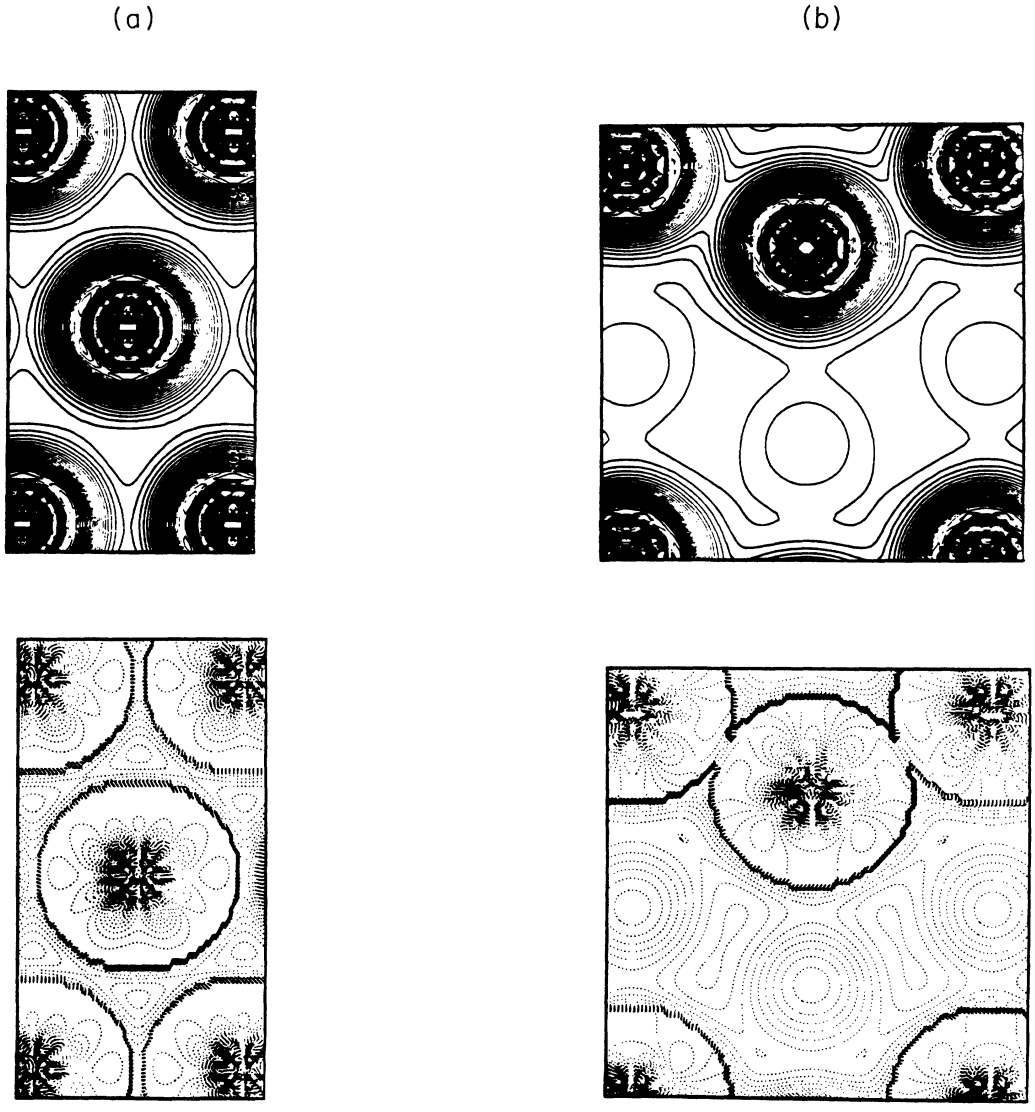

FIG. 6. Charge-density contour plots for orthorhombic Ce (e^-/a.u.^{3}). The contours are cut in the (010) (a) and (100) (b) planes. The contour of the total density is shown in the upper figure, and the contour of the nonspherical density is shown in the lower figure. The spacing between full drawn lines is 0.01 and between dotted lines 0.003.

phase we find that the $5d$ contribution to the eigenvalue sum (not shown) also contributes to driving the transition to that phase. Further evidence of the importance of the $4f$ contribution to the bonding and to determining the crystallographic phases is seen in Fig. 5, where we show the calculated $4f$ and $5d$ occupation numbers for the three structures. "Occupation number," in the context of our calculations, refers to the integrated l-projected density of states (ignoring the interstitial region). Notice that, for all phases, the $4f$ electron count increases with decreasing volume. Notice also that initially the $5d$ occupation numbers are increasing with decreasing volume, analogous to a normal $s \rightarrow d$ transition.[26] However, for low volumes the d count decreases, since for these volumes the f occupation is increasing at the expense of the rest of the valence electrons ($s,p,d \rightarrow f$ transition). Also, Fig. 5 shows that the α' phase has more $4f$ electrons than the α and bct phases at most volumes, but that at volumes corresponding to where that bct phase is stable, the bct phase has the most $4f$ electrons.

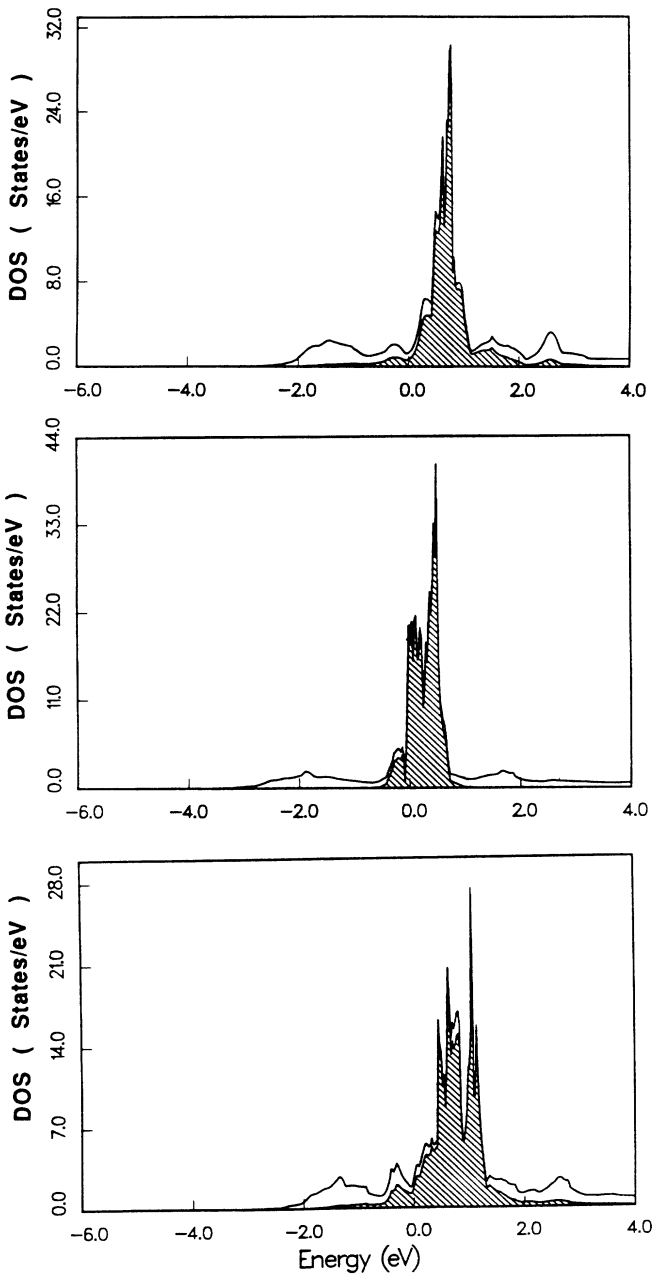

FIG. 7. Calculated DOS using the LMTO-ASA method (Ref. 20). The lower curve is calculated with both hybridization between the $4f$ and the rest of the valence band, as well as the direct $4f$ hopping. The middle curve is calculated without the hybridization term, and the upper curve is calculated without the direct hopping term. The cross-hatched area represents the $4f$ partial DOS. Energies are in eV and the Fermi level is at zero.

CHARGE DENSITY

We have also analyzed the charge-density contours for the different phases at several volumes. The general shape of the charge densities were found to be insensitive to volume. Therefore we consider contour plots for one volume only, 19.96 Å. Furthermore, we show both the total density as well as the nonspherical density, i.e., the density obtained when the spherical component is subtracted out from the total density inside the muffin-tin spheres and the planar average is subtracted out from the interstitial. Notice that since the average interstitial density does not necessarily equal the spherical component at the muffin-tin radius, there will be a "step" in the nonspherical density, which, of course, is absent in the total density. The charge density of the α phase (not shown) is spherically symmetric around the atomic sites and roughly constant in the interstitial region. Similarly, the charge density for bct Ce (not shown) shows that the density to a large extent is spherically symmetric inside the muffin tins. However, the interstitial density cut in the (100) plane reflects the charge density of the underlying atomic plane, since between the atoms in the (100) plane, there is an oval-shaped region (not shown). Finally, the orthorhombic phase shows a more nonsymmetric covalent charge density (Fig. 6). The cut in the (010) plane (a) has a higher overall density than the (100) plane (b). Notice that the charge-density cut in the (100) plane also reflects the atomic positions of the underlying plane, seen in the spherical contours that are in the interstitial region. Furthermore, the nonspherical component inside the muffin-tin regions is more pronounced than in the fcc phase.

HYBRIDIZATION VERSUS DIRECT HOPPING

We have stressed above that the $4f$ electrons play a crucial role for determining the total energies of the low-temperature crystal structures of Ce. The $4f$ contribution to the cohesion in α Ce is in principle accounted for both in the Kondo model[15] (through hybridization only) as well as in the present and previous[10,11,13] calculations. The latter calculations include both hybridization terms as well as direct $4f$-$4f$ hopping. In order to get an estimate of the relative importance of the direct hopping versus hybridization effects for the $4f$ band formation we performed LMTO calculations in the atomic-sphere approximation[20] with the various contributions forced to be zero. The calculated DOS from these calculations are

displayed in Fig. 7. In agreement with previous results,[14] we find that the calculation without $4f$ hopping (upper panel) has a bandwidth that is $\sim 70\%$ of the calculation, which includes all terms (lower panel). The corresponding equation of state underestimates the $4f$ bonding, and the equilibrium volume of α-Ce is ~ 32, Å^3, i.e., close to the γ volume. The bandwidth obtained from the calculation without hybridization (middle panel) is $\sim 85\%$ of the full bandwidth (this can also be estimated by scaling the canonical $4f$ bands with the appropriate potential parameters[20]). This shows that the two contributions are not additive and are about equally important.[14]

CONCLUSIONS

In conclusion, we have, within a band picture, given a good account of the crystallographic phase stabilities in Ce as a function of pressure. This, to our knowledge, is the first time a phase diagram has been successfully calculated for an f-electron system. Moreover, we have shown that the observed $\alpha \rightarrow \alpha'$ transition may be interpreted as being driven by the counterplay between the Madelung term and the $4f$ one-electron term. The $\alpha' \rightarrow$bct transition is somewhat more complex in nature since for this transition the $5d$ electrons also are of importance. However it is equally important to treat the $4f$ electrons as bands, since otherwise the stability range of the bct phase is grossly overestimated. Therefore the contribution of the $4f$ electrons to the bonding is essential in describing the crystallographic phase transitions in Ce under pressure.

ACKNOWLEDGMENTS

Encouragement and valuable discussions with B. Johansson, Uppsala, are acknowledged.

*Present address: Department of Physics, Uppsala University, Uppsala, Sweden.

[1]For a overview, see D. C. Koskenmaki and K. A. Gschneidner, in *Handbook on the Physics and Chemistry of Rare Earths,* edited by K. A. Gschneidner, Jr. and L. Eyring (North-Holland, Amsterdam, 1978). See also A. K. McMahan, J. Less-Common. Met. **149**, 1 (1989).

[2]F. H. Ellinger and W. H. Zachariasen, Phys. Rev. Lett. **32**, 773 (1974); W. H. Zachariasen and F. H. Ellinger, Acta Crystallogr. Sec. A **33**, 155 (1977).

[3]J. Wittig, Phys. Rev. Lett. **21**, 1250 (1968).

[4]The possibility of a related crystal structure of Ce at these pressures has been pointed out in J. Staun Olsen, L. Gerward, U. Benedict, and J.-P. Itie, Physica **133B**, 129 (1985).

[5]E. Wuilland, H. R. Moser, W. D. Schneider, and Y. Baer, Phys. Rev. B **28**, 7354, (1983).

[6]N. Mårtensson, B. Reihl, and R. P. Packs, Solid State Commun. **41**, 573 (1982).

[7]D. R. Gustafson, J. D. McNutt, and L. O. Roellig, Phys. Rev. **183**, 435 (1964); A. M. Boring, C. Y. Huang, K. A. Gschneidner, Jr., J. D. McGervey, M. Pavifrahi, and S. G. Usman, J. Magn. Magn. Mater. **37**, 7 (1983).

[8]N. Kornstädt, R. Lässer, and B. Lengeler, Phys. Rev. B **21**, 1898 (1980).

[9]B. Johansson, Philos. Mag. **30**, 469 (1974).

[10]D. Glötzel, J. Phys. F **8**, L163 (1978).

[11]W. E. Pickett, A. J. Freeman, and D. D. Koelling, Physica **120B**, 341 (1980); B. I. Min, H. J. F. Jansen, T. Oguchi, and A. J. Freeman, Phys. Rev. B **34**, 369 (1986).

[12]M. S. S. Brooks, Physica **130B**, 6 (1985).

[13]O. Eriksson, M. S. S. Brooks, and B. Johansson, Phys. Rev. B **41**, 7311 (1990).

[14]A. M. Boring, R. C. Albers, O. Eriksson, and D. D. Koelling, Phys. Rev. Lett. **68**, 2652 (1992).

[15]J. W. Allen and R. Martin, Phys. Rev. Lett. **49**, 1106 (1982); M. Lavagna, C. Lacroix, and M. Cyrot, Phys. Lett. **90A**, 210 (1982); J. Phys. F **13**, 1007 (1985).

[16]J. W. Allen, S. J. Oh, O. Gunarsson, K. Schönhammer, M. B. Maple, M. S. Torikachrili, and I. Lindau, Adv. Phys. **35**, 275 (1986); J. W. Allen, L. Z. Liu, R. Claessen, R. O. Anderson, J. H. Park, J. S. Kang, C. L. Seaman, M. B. Maple, Y. Dalichaoch, M. D. de la Torre, C. G. Olson, W. P. Ellis, and M. S. Torikachvili (unpublished); J. W. Allen and L. Z. Liu, Phys. Rev. B **46**, 5047 (1992).

[17]J. M. Wills, O. Eriksson, and A. M. Boring, Phys. Rev. Lett. **67**, 2215 (1991).

[18]H. L. Skriver, Phys. Rev. B **31**, 1909 (1985).

[19]J. M. Wills and B. R. Cooper, Phys. Rev. B **36**, 3809 (1987); D. L. Price and B. R. Cooper, *ibid.* **39**, 4945 (1989); J. M. Wills (unpublished).

[20]O. K. Andersen, Phys. Rev. B **12**, 3060 (1975); H. L. Skriver, *The LMTO Method* (Springer-Verlag, Berlin, 1984).

[21]D. J. Chadi and M. L. Cohen, Phys. Rev. B **8**, 5747 (1973); S. Froyen, *ibid.* **39**, 3168 (1989).

[22]O. Gunnarson and K. Schönhammer, Phys. Rev. Lett. **50**, 604 (1983); J. C. Fuggle, M. Campagna, and Z. Zolniereck, *ibid.* **45**, 1597 (1980); S. Höfner and P. Steiner, in *Valence Instabilities,* edited by P. Wachter and M. Boppart (North-Holland, Amsterdam, 1982), p. 263; S. H. Liu and K.-M. Mo, Phys. Rev. B **28**, 4220 (1983); M. R. Norman, D. D. Koelling, A. J. Freeman, H. J. F. Jansen, B. I. Min, T. Oguchi, and L. Ye, Phys. Rev. Lett. **53**, 1673 (1984).

[23]M. Schlüter and C. M. Varma, in *Valence Instabilities* (Ref. 22), p. 259; A. J. Fedro and S. K. Sinha, *ibid.*, p. 371.

[24]E. Weschke, C. Laubschat, T. Simmons, M. Domke, O. Strebel, and G. Kaindl, Phys. Rev. B **44**, 8304 (1991).

[25]O. Eriksson, R. C. Albers, A. M. Boring, G. W. Fernando, Y. G. Hao, and B. R. Cooper, Phys. Rev. B **43**, 4590 (1991).

[26]A. K. Mcmahan, H. L. Skriver, and B. Johansson, Phys. Rev. B **23**, 5016 (1981).

[27]E. Esposito, A. E. Carlson, D. D. Ling, H. Ehrenreich, and C. D. Gelatt, Jr., Philos. Mag. A **41**, 251 (1980).

[28]This analysis is only approximate since we have used the self-consistent potentials in evaluating the one-electron and Madelung contributions to the total energy, in contrast to the more exact analysis of Skriver (Ref. 18) who used the frozen potentials (the force theorem).

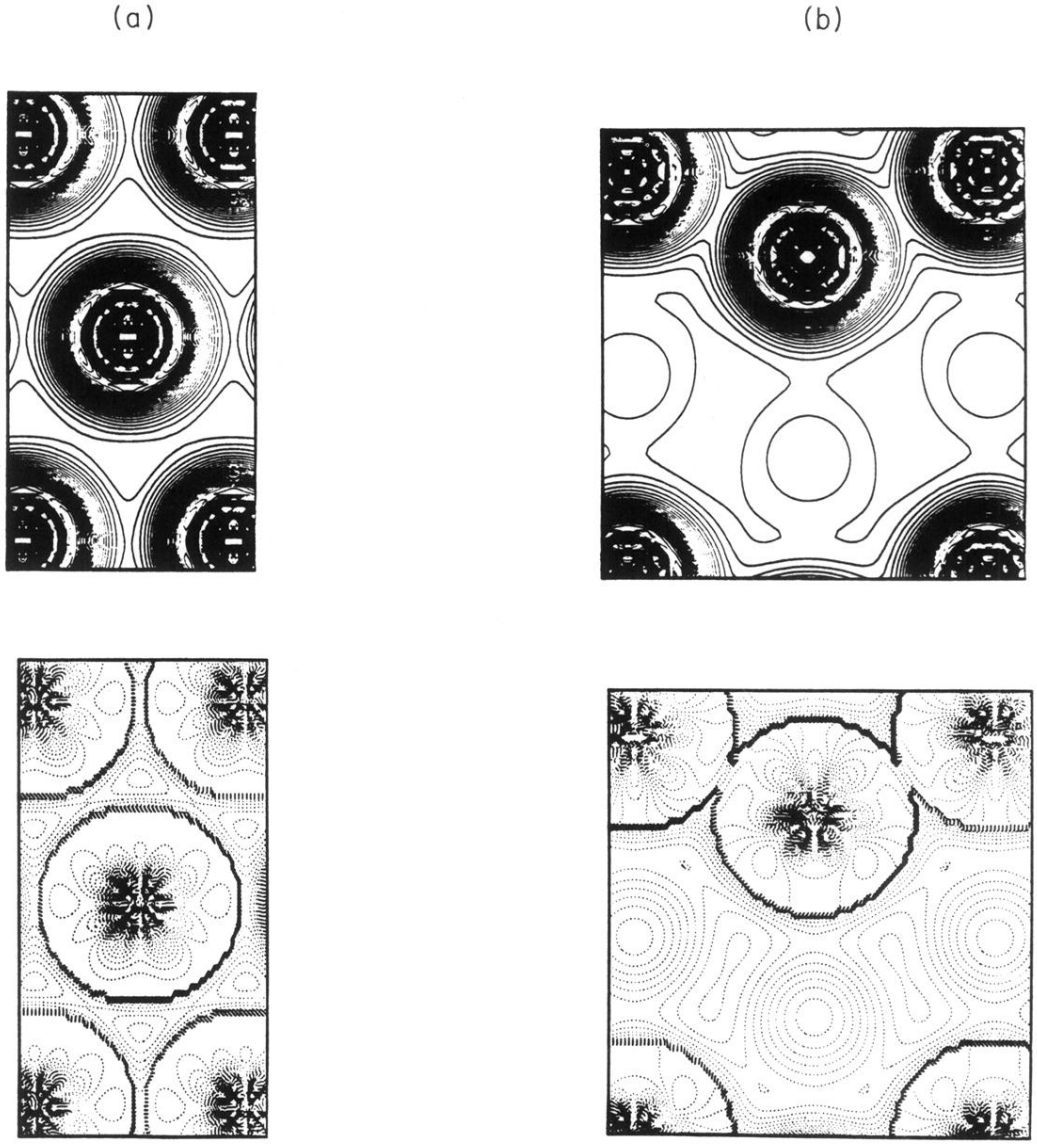

FIG. 6. Charge-density contour plots for orthorhombic Ce (e^-/a.u.^{3}). The contours are cut in the (010) (a) and (100) (b) planes. The contour of the total density is shown in the upper figure, and the contour of the nonspherical density is shown in the lower figure. The spacing between full drawn lines is 0.01 and between dotted lines 0.003.